Biochimica et Biophysica Acta 1838 (2014) 1322–1331

Contents lists available at ScienceDirect

Biochimica et Biophysica Acta

journal homepage: www.elsevier.com/locate/bbamem

Voltage-gated ion channel modulation by lipids: Insights from molecular dynamics simulations

Marina A. Kasimova [a,b], Mounir Tarek [a,c,*], Alexey K. Shaytan [b], Konstantin V. Shaitan [b], Lucie Delemotte [d,**]

[a] Université de Lorraine, SRSMC, UMR 7565, Vandoeuvre-lès-Nancy F-54500, France
[b] Lomonosov Moscow State University, Moscow 119991, Russian Federation
[c] CNRS, SRSMC, UMR 7565, Vandoeuvre-lès-Nancy F-54500, France
[d] Institute of Computational and Molecular Science, Temple University, Philadelphia, PA 19122, USA

ARTICLE INFO

Article history:
Received 5 August 2013
Received in revised form 17 January 2014
Accepted 24 January 2014
Available online 8 February 2014

Keywords:
Sphingomyelin
Ceramide
PIP2
Kv1.2
Shaker

ABSTRACT

Cells commonly use lipids to modulate the function of ion channels. The lipid content influences the amplitude of the ionic current and changes the probability of voltage-gated ion channels being in the active or in the resting states. Experimental findings inferred from a variety of techniques and molecular dynamics studies have revealed a direct interaction between the lipid headgroups and the ion channel residues, suggesting an influence on the ion channel function. On the other hand the alteration of the lipids may in principle modify the overall electrostatic environment of the channel, and hence the transmembrane potential, leading to an indirect modulation, i.e. a global effect. Here we have investigated the structural and dynamical properties of the voltage-gated potassium channel Kv1.2 embedded in bilayers with modified upper or lower leaflet compositions corresponding to realistic biological scenarios: the first relates to the effects of sphingomyelinase, an enzyme that modifies the composition of lipids of the outer membrane leaflets, and the second to the effect of the presence of a small fraction of PIP2, a highly negatively charged lipid known to modulate voltage-gated channel function. Our molecular dynamics simulations do not enable to exclude the global effect mechanism in the former case. For the latter, however, it is shown that local interactions between the ion channel and the lipid headgroups are key-elements of the modulation.

1. Introduction

Voltage-gated potassium channels (VGKCs) are transmembrane (TM) proteins that enable the rapid and coordinated conduction of potassium ions across the cell membrane upon alteration of the TM potential. These channels are homotetramers, each monomer spanning the membrane six times (S1 to S6). The central pore, formed by the assembly of S5 and S6, allows potassium ions to flow. The S1–S4 helix bundles constitute the peripheral voltage-sensor domains (VSDs), which sense the changes in the TM potential and trigger the conformational change responsible for the gating, i.e. opening and closing of the pore. S4 of the VSD contains 4 to 7 positively charged amino acids that sense the electric field and move in response to it. Under depolarizing conditions, S4 transfers upwards (UP), resulting in the channel's activation. When the membrane is hyperpolarized, the electric field causes S4 to move outwards (DOWN), leading to the channel's deactivation and pore closure [1–5].

1.1. Interaction between VGKCs and lipid content

According to the crystal structures of Kv1.2 [6], a mammalian Shaker-like channel, and the Kv1.2/2.1 paddle chimera [7], the VSDs are embedded in the membrane with S4 being mostly shielded away from the lipids. For these channels, S4 carries six positively charged amino acids (R294, R297, R300, R303, R309 and K306 in Kv1.2, called hereafter R1, R2, R3, R4, R6 and K5). Molecular dynamics (MD) simulations of Kv1.2 and Kv1.2/2.1 embedded in lipid bilayers have shown that for the resolved structures, the top gating charges R1 and R2 come in interaction with the lipid headgroups, making stable electrostatic interactions with their negatively charged phosphates. Prior to the crystal structure determination, using site-directed spin labeling and electron paramagnetic resonance spectroscopy, Cuello et al. showed that the S4 segment of the bacterial VGKC KvAP is located at the protein/lipid interface [8]. The same result was obtained by Lee and MacKinnon, studying the action mechanism of a voltage-sensor toxin, VSTX1, from the Chilean Rose Tarantula [9]. Further MD simulations have reported that the positive residues of S4 interact with the headgroups of the lipids. When the activated open state of Kv1.2 was relaxed in a zwitterionic membrane environment, S4 in its 'UP' state position provided the opportunity for the top positive residues (R1 and R2) to interact with the negative charges of the lipid phosphate groups from the outer membrane leaflet [10–15]. Models of the resting/closed state conformation of

* Correspondence to: M. Tarek, Université de Lorraine, SRSMC, UMR 7565, Vandoeuvre-lès-Nancy F-54500, France. Tel.: +33 383 68 43 74.
** Corresponding author. Tel.: +1 215 204 4216.
E-mail addresses: marina.kasimova@univ-lorraine.fr (M.A. Kasimova), mounir.tarek@univ-lorraine.fr (M. Tarek), shaytan_ak@mail.bio.msu.ru (A.K. Shaytan), k.v.shaitan@molsim.org (K.V. Shaitan), lucie.delemotte@temple.edu (L. Delemotte).

0005-2736/$ – see front matter © 2014 Elsevier B.V. All rights reserved.
http://dx.doi.org/10.1016/j.bbamem.2014.01.024

the channel embedded in a model membrane have also shown that the 'DOWN' state position of the S4 helix favors the interaction of the bottom positive residues (R4, K5 and R6) with the headgroups of the lipids from the inner membrane leaflet [16,17]. In the modeling studies that uncovered the entire deactivation pathway, it was found that the top and bottom charges of S4 may interact respectively and simultaneously with the headgroups of the inner and outer membrane leaflets in given intermediate states [4,18–20]. Further experiments demonstrate the important influence of lipid headgroups on VGKC function: reconstitution of a bacterial VGKC KvAP in a positively charged bilayer abolishes the function of the channel [21]. An insight into the molecular level process was provided using MD simulations [22].

1.2. Modulation of VGKCs by the outer membrane leaflet composition

Several experimental findings confirm the fact that the lipid environment may modulate the function of VGKCs. The activation of Shaker is suppressed if the channel is reconstituted in a positively charged bilayer [21]. Also, the removal of the lipid headgroup by some enzymes results in severe modification of the VGKC function through the perturbation of the VSD activation/deactivation [13–15]. In cells, VGKCs are embedded in a complex membrane that is composed of different types of lipids and that is most of the time asymmetrical. Sphingomyelin, a zwitterionic phospholipid, is mainly found in the outer leaflet where it can represent up to 15% of the lipid content in mammalian cells [23]. Enzymes called sphingomyelinases target the headgroup of the sphingomyelin and cut it partly or entirely. Sphingomyelinase D removes the choline group from the lipid, yielding the negatively charged ceramide-1-phosphate and favoring thereby the activated conformation of VGKCs. Another enzyme called sphingomyelinase C removes the entire headgroup, yielding ceramide, a polar lipid that bears no phosphate group to anchor R1 and R2. This causes the closed state of the channel to be preponderant [23–25].

1.3. Modulation of VGKCs by the inner membrane leaflet

Other examples of lipid modulation are known. Phosphatidylinositol-(4,5)-bisphosphate (PIP2) is a negatively charged phospholipid from the inner leaflet of the plasma membrane that was shown to modulate the function of several ion channels. Functional and structural studies have revealed that PIP2 has a major impact on the stabilization of the open state of several potassium channels including KCNQ, hERG, Kir, HCN and TRP channels [26–36], despite its very low concentration in cells (~1%) [37]. The same effect was later found for the channels from the Shaker family [38,39], causing a gain-of-function effect, i.e. an increase in the ionic current. In the same study, a contradictory loss-of-function effect was also shown, manifested by the right shift of the G/V and Q/V curves.

Despite the importance of the lipid modulation in a variety of biological processes, the molecular mechanisms involved still remain elusive. The key stimulus of VGKC activation is changing the TM potential. However several pieces of evidences suggest that mechanical stress, i.e. membrane stretching, also modulates VGKC functions [40–42]. Changes in lipid composition might have a global effect related to membrane lateral tension. This scenario has been discarded in the systems studied here for two main reasons: (1) in the case of sphingomyelin and its products, Lu and collaborators have demonstrated that SMase D effect vanishes after removing charges in S4, supporting the notion that SMase D modification of sphingomyelin molecules alters the electrostatic environment of the VSD [23]; and (2) in the case of PIP2, the concentration of the charged lipids is too low (~1%) [37] to consider an impact on elastic properties of membrane. Accordingly we focus here on elucidating the electrostatic effect of lipid alteration.

To explain the lipid electrostatic effects on VGKCs, two hypotheses may be put forward: 1) altering the lipid headgroups could lead to a modification of the TM potential or a reshaping of the electric field profile through the VSD, an effect that we will call "global"; and 2) it may also change the interactions between the lipid headgroups and the S4 basic residues of the channel locally, an effect that we will therefore refer to as "local". In order to discriminate between the two mechanisms, we resort to atomistic MD simulations.

Specifically, we study the structural and dynamical properties of various states (activated, resting and intermediate) of the voltage-dependent potassium channel Kv1.2 in different lipid environments: in a broadly used zwitterionic bilayer (palmitoyl-oleyl-phosphatidylcholine), in a bilayer with a modified outer leaflet (sphingomyelin (SM) and its products, negatively charged ceramide-1-phosphate (C1P) and polar ceramide (Cer)) and in a bilayer with a modified inner leaflet (PIP2). SM can make up to 15% of the lipid content in specific cells and be involved in a global effect as well as in specific interactions. To investigate thoroughly the effect of altering SM to its products on the TM potential, we have started by studying bare asymmetric bilayer. We have found that going from zwitterionic SM to negatively charged ceramide-1-phosphate (C1P) and to polar ceramide (Cer) does indeed result in a rearrangement of the different components of the system. For C1P, specifically, this results in a noticeable change of the overall transmembrane potential, i.e. when the lipid headgroup nature changes from zwitterionic to charged, hinting to a potential global electrostatic effect. PIP2 lipids, on the other hand, represent only a small fraction of bottom membrane leaflet (~1%) [37] enabling us to rule out a global effect immediately. We have investigated therefore the existence of specific binding pockets for the headgroups of these lipids and identify the specific residues involved. Thus, in this case, we conclude that the specific electrostatic regulation mechanism dictates channel function.

2. Methods

2.1. Preparation of the systems

2.1.1. Bare bilayers

Three bare lipid bilayer systems were built to probe the global effect of lipid modification. All contained 100% palmitoyl-oleyl-phosphatidylcholine (POPC) in the bottom leaflet and 100% of a sphingomyelin-derivative with a palmitoyl-oleyl chain in the upper one: 1— sphingomyelin (SM), 2— ceramide-1-phosphate (C1P) and 3— ceramide (Cer). These bilayers were solvated with a 150 mM NaCl solution. The composition of the systems is presented in Table 1.

2.1.2. Kv1.2 embedded in different bilayers

Systems consisting of Kv1.2 in its open [6], intermediate and closed states [18] were embedded in five different bilayers: 1 — a symmetric POPC bilayer, the entire system was extracted from the previous simulations (see [18], for details); 2, 3, 4 — three sphingomyelin-derivative asymmetric bilayers (SM, C1P and Cer); and 5 — a POPC bilayer in which the inner membrane ring of lipids surrounding the channel was replaced by PIP2.

The channel's conformations were inserted in pre-equilibrated asymmetrical bilayers (SM/POPC, C1P/POPC and Cer/POPC). In order to avoid repulsive contacts, the lipid and water molecules less than 1 Å away from the Kv1.2 were deleted. The systems containing PIP2 ring in the lower bilayer leaflet were constructed using packmol [43]. We have considered a tolerance of 2.0 Å as the minimum distance between packed molecules. All the systems were solvated with water and ionized to 150 mM KCl concentration. For the details of the systems' composition, see Table 2.

2.1.3. Force field parameters

The CHARMM22 force field with CMAP correction was used to build protein topology [44], together with the TIP3P model for water [45]. CHARMM27 and its compatible force fields proposed by Hyvönen and Kovanen [46] were considered for the systems containing

Table 1
Summary table of the three asymmetrical bare bilayer systems (SM/POPC, C1P/POPC and Cer/POPC). For the lipid composition, the first value indicates the number of SM or its derivative molecules; the second value corresponds to the number of POPC molecules.

	Lipid composition	Water molecules	Ions	Total number of atoms	Size (Å^3)
SM/POPC	49/49	5168	56/56	28,895	53 × 56 × 94
C1P/POPC	49/49	5026	72/23	27,570	57 × 48 × 96
Cer/POPC	49/49	5182	49/49	27,845	55 × 52 × 96

sphingomyelin-derivatives. To describe the systems with PIP2, CHARMM36 [47] and its compatible force field developed by Lupyan et al. [48] were applied. The C1P molecules were built by cutting the choline group from SM. The Cer molecules were constructed by cutting the phosphate group from C1P and replacing it by a primary alcohol group.

2.2. MD simulation protocols

Both, NVT and NPT MD simulations (see below), were performed using NAMD [49]. Langevin dynamics was applied to control the temperature (300 K) and the pressure (1 atm). The time-step of the simulations was 2.0 fs. Short- and long-range forces were calculated every 1 and 2 time-steps respectively. Long-range electrostatics was calculated using Particle Mesh Ewald (PME). The cutoff distance of short-range electrostatic calculations was taken to be 11 Å. A switching function was used between 8 and 11 Å to smoothly bring the VdW forces and energies to 0 at 11 Å. The equations of motion were integrated using a multiple time-step algorithm. During the calculations chemical bonds between hydrogen and heavy atoms were constrained to their equilibrium values. Periodic boundary conditions were applied. The simulations were performed on the SGI ALTIX ICE Machine JADE at the CINES supercomputer center (Montpellier, France).

The bare bilayers were equilibrated during 10 ns in the NPT ensemble at 300 K and 1 atm until reaching the stable lateral density. The systems with the channel were relaxed following a standard procedure: first the entire protein was fixed for 6 ns in order to ensure the relaxation of the lipids and the solution. In a second step, the backbone atoms were constrained during 10 ns, enabling subsequent reorganization of the side-chain groups. Finally, all constrains were released and the systems were equilibrated for 20 ns (bare POPC and sphingomyelin-derivative bilayers) and for 100 ns (POPC bilayer with the ring of PIP2 lipids in the lower membrane leaflet). All the relaxation steps were performed in the NPT ensemble at 300 K and 1 atm. The RMSD from the initial structure of the channel calculated for the backbone atoms reached equilibrium values after ~25 ns.

2.3. Charge imbalance method

The TM voltage, ΔV, defined as the difference between the intracellular, bottom, and the extracellular, top, potentials, was set by explicit ion dynamics [50]. In this scheme, air/water interfaces are created on both sides of the electrolytes, by extending the length of the original box in the direction perpendicular to the membrane. The system is then simulated in the NVT ensemble. Note that the density for bulk water is preserved through intermolecular interactions and that as long as the membrane (and protein) is far enough (approximately 25 Å) from the air/water interface, it is not affected by the latter. The charge imbalance (Q) is generated by displacing an appropriate number of K^+ or Cl^- ions from one of the electrolytes to the other, keeping therefore constant the overall concentration of the bulk phases. As the membrane/channel system behaves as a condenser, Q between the electrolytes creates a TM potential ΔV. Using this scheme, the Cer/POPC system containing Kv1.2 was submitted to a 600 mV hyperpolarizing TM potential for >120 ns. The constant volume simulations involved an extended MD cell of 338 Å along the membrane normal.

2.4. Electrostatic potential calculations

The electrostatic potential was calculated by solving the Poisson equation in one dimension where $\rho(Z)$ is the charge distribution along the normal to the membrane Z. Practically, we approximate all point charges by a spherical Gaussian of inverse width β 0.25 Å^{-1}. We calculate the average charge distribution on a 1 Å spaced grid over 100 configurations spread out over 2 ns simulation runs (this

Table 2
Summary table of the eleven systems containing the three Kv1.2 states (open, intermediate and closed) in the four asymmetrical bilayers (SM/POPC, C1P/POPC, Cer/POPC and POPC/PIP2).

	Channel state	Lipid composition	Water molecules	Ions	Total number of atoms	Size (Å^3)
1	Open	SM (319) POPC (331)	84,909	141/97	368,254	153 × 159 × 146
2	Open	C1P (297) POPC (318)	78,345	392/51	338,665	165 × 141 × 142
3	Open	Cer (320) POPC (323)	86,143	143/99	364,923	157 × 148 × 153
4	Open	POPC (368) PIP2 (65)	86,116	613/224	343,436	145 × 145 × 159
5	Intermediate	SM (315) POPC (323)	85,106	142/98	367,227	150 × 152 × 156
6	Intermediate	C1P (313) POPC (320)	75,374	534/177	332,192	157 × 142 × 155
7	Intermediate	Cer (320) POPC (326)	84,482	141/97	359,400	152 × 146 × 158
8	Closed	SM (323) POPC (333)	97,757	159/115	407,650	153 × 151 × 171
9	Closed	C1P (306) POPC (316)	88,136	424/74	368,896	162 × 132 × 167
10	Closed	Cer (326) POPC (323)	84,506	141/97	359,760	155 × 143 × 158
11	Closed	POPC (376) PIP2 (54)	87,465	562/248	346,869	144 × 158 × 156

corresponds to a frame taken every 20 ps) and then calculate the average and the standard deviation from the mean for 15 separate 2 ns runs.

2.5. Gating charge calculations

The calculation of the gating charge (Q) was carried out using the direct method introduced by our group [20,51]. Using the charge imbalance method, if ionic conduction through the channel's pore is prevented, the movement of protein charges across the membrane capacitor is reflected directly by a change in the measured TM potential (ΔV). In practice, the gating charge associated with the conformational change from state λ_1 to λ_2 is written as:

$$Q = \frac{-1}{2}\left[q_0^{protein}(\lambda_2) - q_0^{protein}(\lambda_1)\right].$$

The TM voltage is related to the charge imbalance q_0 between the electrolytes through:

$$\Delta V = \frac{q_0}{AC},$$

where A is the membrane area and C is the membrane capacitance. q_0 arises from the contribution of both, ions ($q_0{}^{ion}$) and protein ($q_0{}^{protein}$):

$$q_0 = q_0^{protein} + q_0^{ion}.$$

As C is constant for a channel/membrane system in the TM voltage range considered [51,52], this allows one to combine the previous equations to write $q_0{}^{protein}$ as

$$q_0^{protein} = -q_0^{ion} + AC\Delta V.$$

As $q_0{}^{ion}$ is maintained fixed, variations in ΔV are then directly linked to the protein gating charge.

For the calculation of the gating charge of three Kv1.2 transitions (activated/intermediate, intermediate/resting and activated/resting), two 2 ns simulations of the three systems are used: one under a transmembrane potential of 0 mV and a second one under a positive transmembrane potential (using the charge imbalance/constant volume methodology, see Section 2.3). An extra simulation at a different positive ΔV was performed to check the linear relationship between $q_0{}^{protein}$ and ΔV. A harmonic potential was applied to all the protein atoms to prevent side chain fluctuations. Thus, only the lipids and solution are allowed to rearrange. The electrostatic potential from the two runs was estimated using 100 frames spread over the 2 ns trajectory following the procedure described in Section 2.4.

3. Results

3.1. Kv1.2 in a POPC bilayer: state-dependent interaction

First we describe here the interactions of the Kv1.2 channel with the surrounding lipids considering the channel conformations obtained in a previous study [18]. In particular we focus on the interactions between the positive charges carried by S4 and the lipid headgroups for several conformations sampled by the VSD when going from open/activated to closed/inactivated states. Bilayers formed of zwitterionic lipids (POPC) that bear negatively charged phosphate groups linked to positively charged choline groups were used to mimic eukaryotic plasma membranes.

When embedded in these bilayers, several S4 positive residues of the Kv1.2 channel are in close proximity to the lipid headgroups both in the open/activated and in the closed/resting states of the channel. In the activated state, when the S4 helix is in its 'UP' position, the outermost positive residues R1 and R2 directly interact with the POPC phosphate groups of the outer membrane leaflet (Fig. 1A). The average distances between the nitrogen atoms of the guanidine groups of R1 and R2 and the phosphorus atoms of the POPC phosphate groups are ~5 and 7 Å respectively allowing the formation of salt bridges. In the resting state, when S4 in its 'DOWN' position, the lower positive residues R4, K5 and R6 are in interaction with the lipid headgroups of the inner membrane leaflet (Fig. 1B). The mean distances between the nitrogen atoms of the R4 and R6 guanidine groups and the phosphorus atoms of the POPC phosphate groups are ~7 and 5 Å respectively.

While the interaction between the S4 residues and the membrane lipids for both 'UP' and 'DOWN' states of the Kv1.2 VSD has been also underlined by other groups [5–9], here we have investigated these interactions in the intermediate states of the VSD. In the so-called intermediate state (called as γ in the original paper), we found that the top (R1) and the bottom (R6) positive residues of S4 are in interaction with the phosphate groups of the outer and inner membrane leaflets respectively [18] (Fig. 1C). Note that once the salt bridges between the S4 positive residues and adjacent lipid headgroups are established, they remain stable during the MD simulation time (15 ns) in all of the investigated states [18].

Hence, in addition to the well-known negative residues of S1, S2 and S3 of the VSD that form salt bridges with S4 positive residues and stabilize its conformation in a given state, other binding sites are provided by the phosphate groups of the lipids surrounding the channel in the outer and inner membrane leaflets. The specific salt bridges formed between S4 and the lipids are shown to be state dependent.

3.2. Systems with sphingomyelin-derivative bilayers. Global effect

SM is mostly found in the outer leaflet of the plasma membrane where it can make up to 15% of the lipid content in several cell types [23]. This lipid is the target of specific enzymes called sphingomyelinases that can cut its headgroup partially or entirely. Sphingomyelinase (SMase) D chops off the SM choline group, yielding a negatively charged C1P. SMase C, on the other hand, hydrolyzes the SM headgroup into a Cer that bears no phosphate group. These two enzymes have been shown to facilitate respectively either activation or deactivation of VGKCs [23–25].

To account for the effect of SMases and therefore the presence of SM vs. its products on the function of VGKCs, one should consider two scenarios. In the first one (global effect), modification of the lipid headgroups results in the modulation of the overall electrostatic environment surrounding the channel. In the second scenario (local effect) this modification leads to the change of salt bridge network between the S4 positive residues and the lipids.

In order to enhance the effect due to the lipid headgroup modification, we have chosen asymmetrical bilayers with 100% SM, C1P or Cer in the outer leaflet. This also ensures that specific lipids will interact directly with the top S4 positive charges, which is in agreement with experimental hypotheses. Indeed, in cells, such as *Xenopus* oocytes, SM is suggested to interact preferably with the Kv channel VSDs in comparison to other lipids such as POPC [25].

3.2.1. Estimation of the electrostatic potential profile

In order to probe the global effect, first we determined the overall resting TM potential for the systems of bare bilayers. The electrostatic potential (EP) profiles for SM/POPC, C1P/POPC and Cer/POPC systems are shown in Fig. 2. As expected, all the profiles are virtually identical for the lower leaflet region containing POPC. Similarly to what is found in symmetrical POPC bilayers the overall contribution from the lipid headgroup dipoles is partly canceled out by the reorientation of water molecules and ion reorganization at the membrane/solution interface [53–57]. The total so-called dipole potential of the inner leaflet, i.e. the potential difference between the inner solution and the membrane center, is ~1 V which is consistent with previous simulations using similar force fields [58–61]. In the SM/POPC system zwitterionic

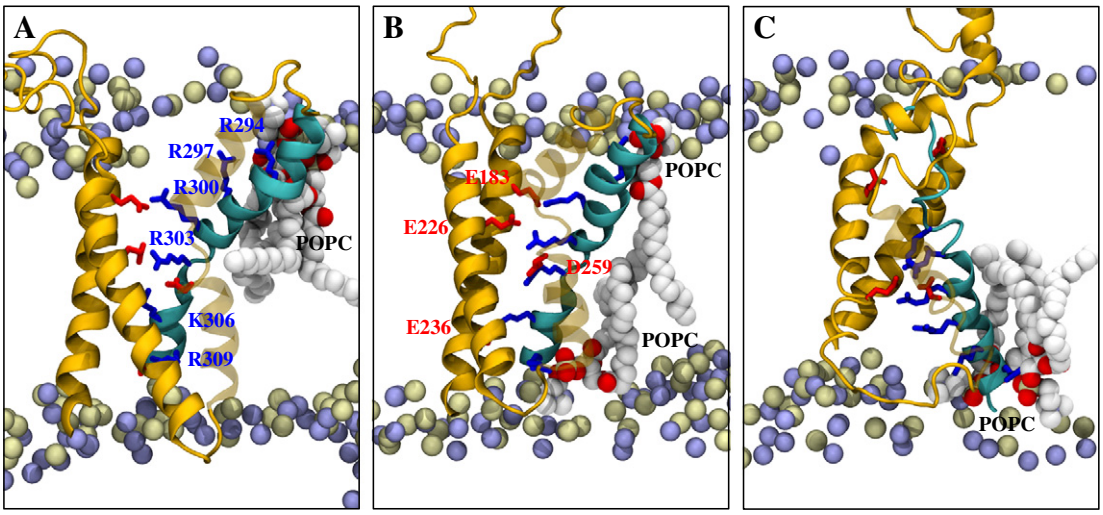

Fig. 1. Kv1.2 embedded in a POPC bilayer (only one VSD is shown). A: Kv1.2 is in the active state. The upper residues of S4, R293 and R297 form salt bridges with the adjacent phosphate groups of the lipid heads from the upper bilayer leaflet. R300, R303, K306 and R309 interact with the negatively charged residues of S1, S2 and S3 helices (E183, E226, E236 and D259). B: Kv1.2 is in an intermediate state. The upper and bottom positive residues of S4, R293 and R309 interact with both bilayer leaflets. C: Kv1.2 is in the resting state. R303, K306 and R309 form salt bridges with the lipid phosphate groups from the bottom bilayer leaflet. S1, S2 and S3 helices are shown in orange, S4 is shown in cyan. The lipid nitrogen and phosphorus atoms are shown as purple and yellow spheres respectively.

SM behaves as POPC, but its headgroups are slightly more polarized. The net TM potential, resulting from the contributions of all the system components, i.e. lipids, water and ions, amounts to ~60 mV. For the C1P/POPC system, since each ceramide-1-phosphate headgroup bears a negative charge, a huge positive contribution to the dipole potential arises, which is partly counter-balanced by an excess of positive sodium ions accumulating at the interface. The resulting total net TM potential amounts to ~130 mV. The ceramide lipids (Cer/POPC system) give rise to an EP contribution with an opposite polarity to the one for SM. However, ion reorganization and water polarization tend to reduce this potential displaying a positive contribution. Quite interestingly, the net TM potentials evaluated from the MD simulations amount to ~60 mV, equivalent to the SM/POPC system. Note, however, that the error bars on these measurements (arising mainly from the effect of the fluctuation of the lipid and water dipole contributions in these small patches) are ~50 mV and that while we can expect the tendency to be conserved, the absolute magnitude of the TM potential is likely to be sensitive to the force field employed.

3.2.2. Calculation of the gating charge

To further probe whether the global effect hypothesis could explain the change in the channel function, we have embedded the Kv1.2 channel in the three asymmetrical bilayers, SM/POPC, C1P/POPC and Cer/POPC (Fig. 3A and B). We have considered 3 conformations: activated/open, intermediate and resting/closed to characterize the electrostatic environment of the VSDs (the conformations were taken from a previous investigation, see [18]). The latter is known to account for a specific electric field along the VSD, a crucial ingredient of the electromechanical coupling that controls the VSD conformational change through the specific motion of the S4 charges [18]. Hence, to probe the alteration of the electric field along the VSD indirectly, we have calculated the gating charge values (Q) associated with the transition from the activated to the intermediate and resting states. The latter were estimated using the direct measurement protocol [51] (Table 3). The value of the gating charge corresponding to the activated/open to inactivated/close transition in all the probed systems remains unmodified (3.1 ± 0.3 to 3.5 ± 0.3e) indicating indirectly that the electrostatic environment around the VSDs is not dramatically altered by the change in lipid content.

3.3. Systems with sphingomyelin-derivative bilayers. Local effect

In order to probe the local effect of lipid modification on the channel activation, we have investigated the activated/open, intermediate and resting/closed states embedded in the asymmetrical bilayer systems (see Section 3.2.2). All three conformations were shown to be stable on the tens of nanosecond time scale enabling the characterization of the salt bridge network within the VSD and between the VSDs and the lipids.

In the systems consisting of the different states of Kv1.2 embedded in the SM/POPC bilayer, as expected from the zwitterionic nature of SM, the salt bridge network between the lipids and the channel is comparable to the one found in POPC and remains stable for over 20 ns. In the activated state, R1 and R2 are found to be close to the SM headgroups, while R3, R4, K5 and R6 are engaged in salt bridges with the negatively charged residues from S1 (E183) S2 (E226 and E236) and S3 (D259). In the intermediate state, R1 remains in contact with the lipid headgroups of the top leaflet of the bilayer, R2 to K5 – with the protein negatively charged residues and R6 – with the lipid headgroups of the bottom leaflet. In the resting state, R1, R2 and R3 are located in TM position and interact with the VSD negatively charged residues. R4, K5 and R6, on the other hand, are all in interaction with the POPC headgroups of the bilayer lower leaflet.

In the C1P/POPC systems, the VSDs are surrounded by the negatively charged C1P headgroups in the outer membrane leaflet. As expected from the stronger interaction between R1 and R2 and the negative headgroups of C1P in the activated state (respectively R1 in the intermediate one), the salt bridge network does not reorganize. In the resting state, contrary to what we expected from the excess of negative charges at the top membrane/solution interface, the salt bridge network does not rearrange during the 20 ns of the simulations.

Finally, as Cer is neutral and does not bear any charged moiety in the headgroup, the lipids of the Cer/POPC bilayer do not provide any negatively charged binding site as a stabilizing counter charge for S4 upper residues. Interestingly, starting from the same configurations as in the other systems the salt bridge network remains stable in

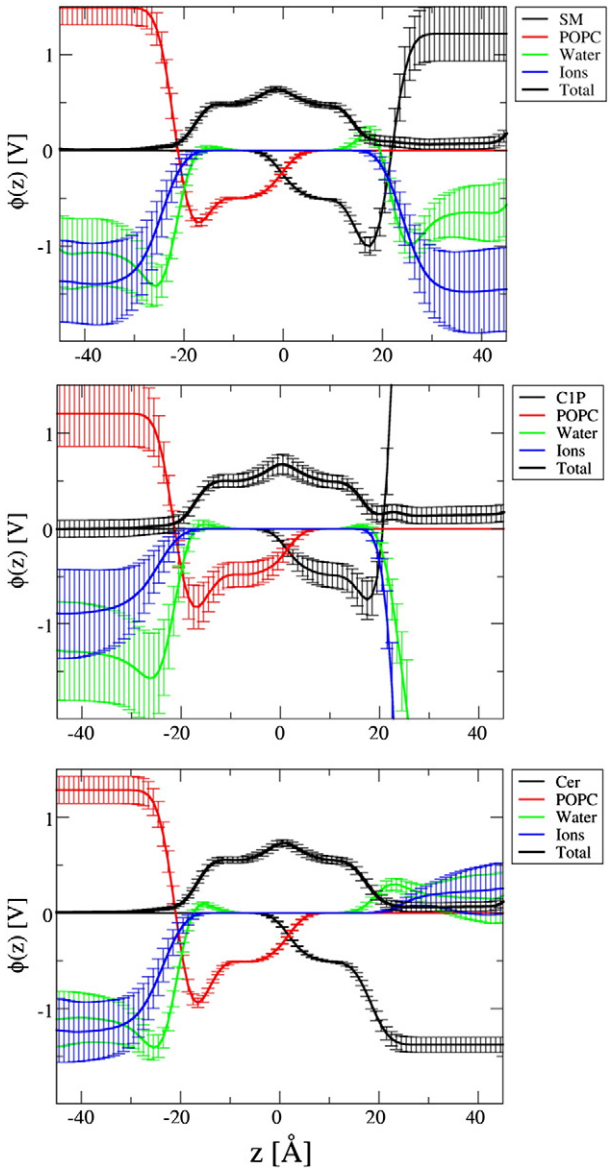

Fig. 2. Electrostatic potential (EP) profiles along the membrane bilayer normal of the modified upper leaflet systems. The profiles are centered at the bilayer center. The mean and standard deviation from the mean were calculated from 15 separate 2 ns simulations. Contributions from the upper leaflet lipids, lower leaflet lipids, water and ions are shown in black, red, green and blue lines respectively. The sum of all contributions is figured as thick dashed lines. A: SM/POPC system. B: C1P/POPC system. C1P lipids bear a net negative charge (−1e), which is why the EP diverges toward positive potentials. Similarly, counterions (Na^+) accumulating at the bilayer/solution interface and polarization of water give rise to diverging negative contributions. C: Cer/POPC system.

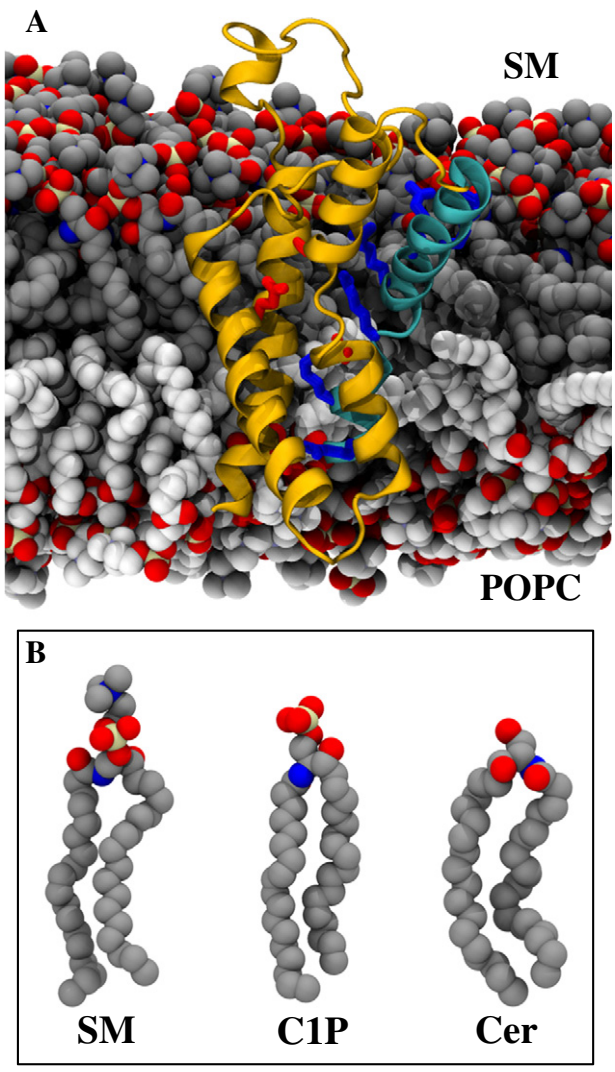

Fig. 3. Kv1.2 is embedded in the bilayer with a modified upper leaflet. A: Kv1.2 in the SM/POPC bilayer. The upper and bottom leaflets are formed of SM and POPC lipids respectively. SM lipids are shown in gray, POPC lipids are shown in white. B: SM, C1P and Cer lipids. The C1P molecule is constructed by cutting the choline group from SM. In order to build the Cer molecule, the phosphate group from C1P is replaced by a primary alcohol group.

two states within 20 ns run. In the open state especially, we expected the salt bridges to reorganize to let the top basic residues R1 and R2 come in contact with the first binding site within the VSD. However no transfer of R1 and R2 occurs even over 120 ns, under a 600 mV hyperpolarized TM potential.

Here, as in the system with the symmetrical POPC bilayer, the S4 positive residues were not found to switch between adjacent lipid headgroups of the top or bottom bilayer leaflets in any of the considered systems.

Altogether, on the tens of nanosecond timescale, no dramatic reorganization of the VSD salt bridge network occurs after alteration of the top leaflet lipid headgroups. The current limits of the investigated simulation times are far too short for an estimate of lifetimes of lipid–protein interactions. Even if the VSD is not in its most stable conformation, breaking the electrostatic interactions may also involve overcoming high free energy barriers. The substantial reorganization of the salt bridge network involving the VSD positive residues may then occur on a time scale that is beyond our current reach.

3.4. Kv1.2 embedded in inner membrane PIP2 lipids

PIP2 is a minor component of cell membranes, accounting for less than 1% of the total lipids of the inner leaflet [37]. Recently it was

Table 3
Gating charge (Q) associated to the conformational changes of the Kv1.2 channel in the three asymmetric bilayers. The gating charge is calculated using the direct measurement method. The values are estimated at ±0.3e due to an estimated 0.05 V error on the TM voltage.

	Q (activated/intermediate) [e]	Q (intermediate/resting) [e]	Q (activated/resting) [e]
SM/POPC	−1.0	−2.5	−3.5
C1P/POPC	−0.9	−2.2	−3.1
Cer/POPC	−1.0	−2.4	−3.4

shown that this highly negatively charged lipid has a measurable dual effect on Shaker family channels [38,39]. Addition of PIP2 to patch-clamp cells results in an increase of ionic current (gain-of-function effect), and vice versa, depletion of PIP2 leads to a decrease of ionic current. Concomitantly, addition of PIP2 also triggers a right-shift of G/V and I/V curves and slows down the kinetics of activation (loss-of-function effect).

Due to the extremely low concentration of PIP2 in cell membranes, we can rule out the hypothesis of a global change in the electrostatic environment, i.e. a global effect of PIP2 on VGKC function. We sought therefore to gain a molecular insight into the PIP2 dual effect on Shaker function by investigating the interaction between the charged lipid and the Kv1.2 channel, which serves as a prototype for other VGKCs such as Shaker. We studied two systems involving the activated and resting state structures of Kv1.2 embedded in a POPC bilayer that contains a ring of PIP2 molecules surrounding the channel in the inner leaflet (Fig. 4A).

3.4.1. Kv1.2 in the resting state

In the resting state, as expected from the fact that PIP2 lipids bear a high negative charge, within 40 ns of unconstrained MD simulations we observed the formation of salt bridges between the bottom positive residues of S4 (R4, K5 and R6) and the PIP2 lipid headgroups. After this initial formation, the salt bridges did not rearrange during a 61 ns simulation, indicative of their stability. Specifically, in three out of four subunits, bottom S4 charges interact with two inositol phosphate groups of PIP2, while in the last subunit, they are in interaction with the phosphate group linking the inositol and the glycerol groups. In all four subunits, the PIP2 molecule that was found in interaction with S4 was also recognized to interact with the positive residue located in the middle of the S4–S5 linker, namely K322 (Fig. 4B). An excess of positive charges arises therefore from the proximity of the positive residues of the S4–S5 linker and of the bottom of S4, forming a binding pocket for highly negatively charged PIP2 molecules.

In addition to this binding site, three out of four PIP2 molecules were found to interact with K312 and R326 located each at one end of the linker. One of these PIP2 molecules interacts with K312 and R326 simultaneously, linking two adjacent subunits. In the two other subunits, two different PIP2 molecules interact with the two external positive residues of the linker preventing the formation of the salt bridge network between the channel subunits.

3.4.2. Kv1.2 in the activated state

In the activated state, however, the S4 helix is in its 'UP' position and no positive residues from S4 are engaged in electrostatic interactions with PIP2 lipid headgroups of the inner leaflet. In this state, as is the case in the resting one, PIP2 interacts with K322. In contrast with the resting state, however, the same molecule interacts also with the positive residue of the S6 helix terminus (R419) (Fig. 4C). PIP2 comes indeed as close as 8 Å to R419 in three of the channel subunits starting from

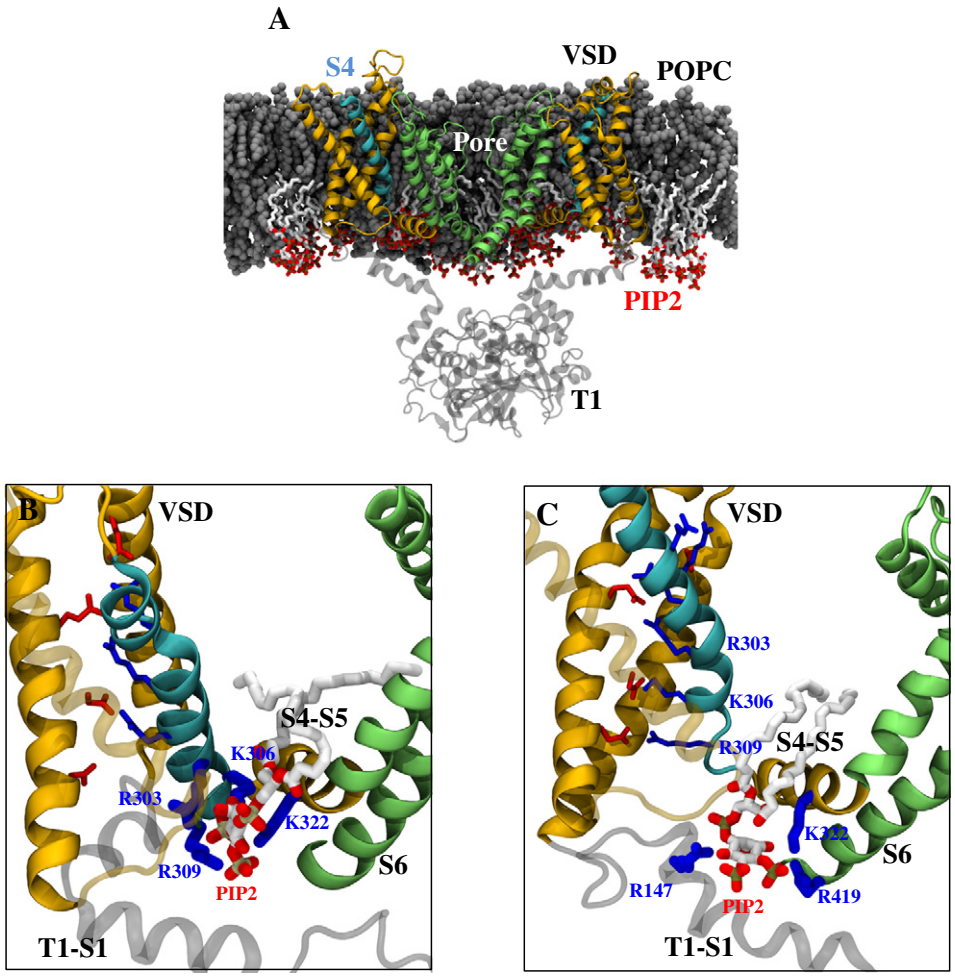

Fig. 4. Kv1.2 in the system containing a ring of PIP2 lipids in the bottom leaflet. A: Side view of the entire system. The pore domain, the VSDs and T1 of Kv1.2 are shown in green, orange and silver respectively. Oxygen and phosphorus atoms of PIP2 phosphate groups are shown in red and brown, respectively. B: The PIP2 binding site in the resting/closed state of the channel. PIP2 interacts with the three bottom residues of S4 (R303, K306 and R309) and with K322 of the S4–S5 linkers. C: The PIP2 binding site in the active/open state of the channel. In the active/open state, PIP2 remains in interaction with K322 of the S4–S5 linkers and attracts the R419 residue of the S6 terminal. Another residue of T1–S1 linkers participates in the formation of the binding site.

40 ns and stays at this distance until the end of the MD simulations. In addition, after ~80 ns, in one of the subunits a positive residue of the T1–S1 linker (R147) comes in close contact with the PIP2 molecule. Altogether in this subunit, the three residues K322, R419 and R147 form a binding pocket for the PIP2 molecule. One may hypothesize that longer simulation times would enable the three other subunits to also reach this optimal configuration.

The interaction between PIP2 molecules and the outermost residues of the S4–S5 linker, K312 and R326, remains in the activated state. However, here, a single PIP2 molecule interacts with both positive residues linking adjacent subunits in three out of four cases (after 80 ns of calculations). This could be a key interaction in stabilizing the position of the linkers and therefore the open conformation of the pore.

3.4.3. Rationalization of the dual effect of PIP2

Overall, our data provides a molecular model that rationalizes the dual effect of PIP2 lipids on the channels of the Shaker family: from the MD simulations carried out here, it appears that the PIP2 molecules of the inner membrane leaflet interact with the Kv1.2 channel in a state-dependent manner. In the closed state, PIP2 anchors positive residues of the S4–S5 linkers and interacts simultaneously with the bottom residues of S4 stabilizing its 'DOWN' position and thereby the resting state of the channel. In the open state, the PIP2 molecules are still in contact with the S4–S5 linkers but they exchange their neutralizing counterparts by engaging in an interaction with the positive residues of the S6 terminus. This stabilizes therefore the open state of the channel, possibly through a mechanism similar to that described for Kir channels [34]. In addition, PIP2 seems to act on the inter-subunit contact between the S4–S5 linkers in the open state by interacting with their outermost positive residues, possibly stabilizing further the open state of the pore.

4. Discussion

The modification of the lipid headgroups can modulate VGKC function as shown by several elegant electrophysiology measurements. Two hypotheses that may explain this modulation are as follows: the global effect mechanism hypothesizes that different lipids may give rise to different electrostatic environments, which could result in the modification of the resting TM potential. Additionally, lipid modification can also reshape the electric field around the channel and as a result induce measurable changes of the gating charge. The local effect mechanism, on the other hand, stems from the rearrangement of the salt bridges between the protein positive residues and the surrounding lipids when the chemical nature of the latter is modified.

4.1. Lipid modulation by sphingomyelinase may involve a global effect

Changes in the lipid headgroups between SM, C1P and Cer modify the individual contribution of the system components to the total TM potential, and in the case of C1P, alter the resting transmembrane potential (from 60 ± 50 mV to 130 ± 50 mV). The lipid composition, and in particular the concentration of SM or its products considered here (100% lipid content of the upper leaflet) are much higher than under physiological conditions where SM can make up ~15% of the lipid content in mammalian cells. However, SM may aggregate at the vicinity of VGKCs leading to a higher local concentration. Accordingly, while the gating charge values estimated for the activation of Kv1.2 are hardly modified by the changes in the lipid composition, a global effect, at least in the case of C1P, cannot be ruled out to rationalize alteration of VGKC function. The brute force MD simulations were not successful in proving that the lack of phosphate groups leads to significant destabilization of the state dependent interactions (or lack thereof) between the negatively charged phosphate moiety of the lipid and the positive charges of S4. The simulation time scale investigated in the present study appears to be too short to probe the lifetime of lipid–protein specific interactions. We will need to extend this work and most likely resort to enhanced sampling methods to characterize thoroughly the modification of the free energy landscape of VGKC activation by the exchange of external leaflet lipids.

4.2. Stabilization of the channel pore by PIP2

In the second part, we have shown that PIP2 interacts directly with the distal positive residues of S6 helix that is located at the level of the membrane/solution interface if the channel is in its activated state. This is consistent with the experimental results showing that mutations of S6 positive residues significantly reduce PIP2 affinity for Kv channels [62]. One experimental finding that we cannot reconcile with our model, though, is the increase of ionic current of the R419Q mutant in the presence of PIP2 [39]. However, the entire mechanism of activation (including all the intermediate steps) affected by these lipids remains elusive. One can suggest two possible mechanisms by which the interaction between PIP2 and Kv channels results in the stabilization of the open channel structure.

- The activation of the VSDs results in the increasing of the volume enclosed between the S4–S5 linkers and allows thereby, in the case of a weak coupling between the VSDs and the pore, fluctuations of the gate between its closed and open conformations. In the absence of PIP2, these fluctuations lead the open state to be short-lived and result in a small ionic current. Application of PIP2 on the other hand will link the distal positive residues of S6 with the membrane and stabilize thereby the channel open state and enhance ionic current flow through the pore.
- In the second hypothetical mechanism, PIP2 enhances rather the coupling between the VSDs and the channel gate. Here, we posit that PIP2 couples the movement of S4 tightly with the S6 gating process. In the absence of PIP2, a depolarized voltage leads to the activation of the VSDs only, whereas the gate of the channel remains closed. In the presence of PIP2 on the other hand, upward movement of S4, even if made more difficult by the presence of PIP2, drags S6 closer to the membrane and favors the channel opening.

The crucial difference between the two proposed mechanisms is the following: while the second one requires PIP2 binding site partly formed by the S4–S5 linkers, the first mechanism involves positive residues of S6 only. Therefore channels lacking a voltage-sensor domain can use this mechanism when PIP2 is present in the system, as seen for Kir channel family. Functional and structural studies have revealed that PIP2 binds with a specific site of Kir composed of a cluster of positive residues on the inner and outer TM helices [28,29,34], which correspond to S6 and S5 of Kv1.2, respectively. According to two crystal structures, binding of PIP2 leads to a chain of conformational changes in the channel resulting in its opening [28,34]. Notably, the residues involved in PIP2 binding that were predicted by MD simulations are in a good agreement with the experimental data [63].

The PIP2 state-dependent binding site uncovered in this work seems to have been designed for the coupling purpose (the second mechanism), as it is composed of the positive residues from the bottom of S4, the distal part of S6 and the S4–S5 linkers: in the open state, specifically, a single PIP2 molecule interacts simultaneously with the gate of the channel and its linker. This mechanism has recently been suggested for Kv7.1 but the specific residues involved in the process remain to be identified [36,64].

4.3. Modulation of the VSD by PIP2 lipids

As experimentally evidenced, PIP2 leads to a loss-of-function effect in Shaker channels, manifested by a right shift of G/V and Q/V curves. This effect was attributed to the VSD because of the voltage-dependence change upon PIP2 application. In this work, we have demonstrated that PIP2 directly interacts with the bottom positive residues of S4 when the channel is in its closed state.

Other voltage-dependent channels were shown to be sensitive to the presence and concentration of PIP2. Among them, sea urchin hyperpolarization-activated cyclic nucleotide-gated channel (HCN) SpIH shares significant sequence homology with voltage-gated potassium channels. SpIH gating, however, has an opposite dependence on the membrane potential as hyperpolarization causes the opening of the gate. Functional studies have revealed that the binding of PIP2 to SpIH has a potentiation effect, manifested by a left shift in the voltage dependence of activation [27]. This effect was linked to the transmembrane region of the channel because PIP2 produced shifts in the voltage dependence of full-length and truncated channels (without the N- and C-terminal domains). SpIH S4 helix carries five positive residues that can sense variations in the TM potential. As the channel activates under hyperpolarized voltages, S4 is likely moving down during the process of gating and the 'DOWN' position of the S4 helix, in which it can in principle interact with lipid headgroups of the inner membrane leaflet, corresponds to the VSD active state. The PIP2-dependent left shift of the voltage-dependence of activation can be explained by the stabilization of the VSD in its 'DOWN' position. Thus, depending on the working mechanism of the channel, inner leaflet PIP2 can cause either a right shift of the voltage-dependence of the activation as in Kv1.2 or a left shift as in SpIH.

Acknowledgements

This work was performed using HPC resources from GENCI-CINES (grant nos. c2011075137, c2011076742). L.D. receives funding from the European Union Seventh Framework Programme (PIOF-GA-2012-329534).

References

[1] F. Bezanilla, The voltage sensor in voltage-dependent ion channels, Physiol. Rev. 80 (2000) 555–592.
[2] W.A. Catterall, Ion channel voltage sensors: structure, function, and pathophysiology, Neuron 67 (2010) 915–928.
[3] R. Mackinnon, Structural biology. Voltage sensor meets lipid membrane, Science 306 (2004) 1304–1305.
[4] M. Tarek, L. Delemotte, Omega currents in voltage-gated ion channels: what can we learn from uncovering the voltage-sensing mechanism using MD simulations? Acc. Chem. Res. 46 (2013) 2755–2762.
[5] B. Hille, Ionic Channels of Excitable Membranes, 3rd ed. Sinauer Associates, Sunderland, MA, 2001.
[6] S.B. Long, E.B. Campbell, R. MacKinnon, Crystal structure of a mammalian voltage-dependent Shaker family K^+ channel, Science 309 (2005) 897–903.
[7] S.B. Long, X. Tao, E.B. Campbell, R. MacKinnon, Atomic structure of a voltage-dependent K^+ channel in a lipid membrane-like environment, Nature 450 (2007) 376–382.
[8] L.G. Cuello, D.M. Cortes, E. Perozo, Molecular architecture of the KvAP voltage-dependent K^+ channel in a lipid bilayer, Science 306 (2004) 491–495.
[9] S.-Y. Lee, R. MacKinnon, A membrane-access mechanism of ion channel inhibition by voltage sensor toxins from spider venom, Nature 430 (2004) 232–235.
[10] P. Bjelkmar, P.S. Niemelä, I. Vattulainen, E. Lindahl, Conformational changes and slow dynamics through microsecond polarized atomistic molecular simulation of an integral Kv1.2 ion channel, PLoS Comput. Biol. 5 (2009) e1000289.
[11] J.A. Freites, D.J. Tobias, G. von Heijne, S.H. White, Interface connections of a transmembrane voltage sensor, Proc. Natl. Acad. Sci. U. S. A. 102 (2005) 15059–15064.
[12] V. Jogini, B. Roux, Dynamics of the Kv1.2 voltage-gated K^+ channel in a membrane environment, Biophys. J. 93 (2007) 3070–3082.
[13] Z.A. Sands, M.S.P. Sansom, How does a voltage sensor interact with a lipid bilayer? Simulations of a potassium channel domain, Structure 1993 (15) (2007) 235–244 (England).
[14] W. Treptow, M. Tarek, Environment of the gating charges in the Kv1.2 Shaker potassium channel, Biophys. J. 90 (2006) L64–L66.
[15] L. Monticelli, K.M. Robertson, J.L. MacCallum, D.P. Tieleman, Computer simulation of the KvAP voltage-gated potassium channel: steered molecular dynamics of the voltage sensor, FEBS Lett. 564 (2004) 325–332.
[16] F. Khalili-Araghi, V. Jogini, V. Yarov-Yarovoy, E. Tajkhorshid, B. Roux, K. Schulten, Calculation of the gating charge for the Kv1.2 voltage-activated potassium channel, Biophys. J. 98 (2010) 2189–2198.
[17] E. Vargas, V. Yarov-Yarovoy, F. Khalili-Araghi, W.A. Catterall, M.L. Klein, M. Tarek, et al., An emerging consensus on voltage-dependent gating from computational modeling and molecular dynamics simulations, J. Gen. Physiol. 140 (2012) 587–594.
[18] L. Delemotte, M. Tarek, M.L. Klein, C. Amaral, W. Treptow, Intermediate states of the Kv1.2 voltage sensor from atomistic molecular dynamics simulations, Proc. Natl. Acad. Sci. U. S. A. 108 (2011) 6109–6114.
[19] M.Ø. Jensen, V. Jogini, D.W. Borhani, A.E. Leffler, R.O. Dror, D.E. Shaw, Mechanism of voltage gating in potassium channels, Science 336 (2012) 229–233.
[20] L. Delemotte, M.L. Klein, M. Tarek, Molecular dynamics simulations of voltage-gated cation channels: insights on voltage-sensor domain function and modulation, Front. Pharmacol. 3 (2012) 97.
[21] D. Schmidt, Q.-X. Jiang, R. MacKinnon, Phospholipids and the origin of cationic gating charges in voltage sensors, Nature 444 (2006) 775–779.
[22] M. Andersson, J.A. Freites, D.J. Tobias, S.H. White, Structural dynamics of the S4 voltage-sensor helix in lipid bilayers lacking phosphate groups, J. Phys. Chem. B 115 (2011) 8732–8738.
[23] D.J. Combs, H.-G. Shin, Y. Xu, Y. Ramu, Z. Lu, Tuning voltage-gated channel activity and cellular excitability with a sphingomyelinase, J. Gen. Physiol. 142 (2013) 367–380.
[24] Y. Ramu, Y. Xu, Z. Lu, Enzymatic activation of voltage-gated potassium channels, Nature 442 (2006) 696–699.
[25] Y. Xu, Y. Ramu, Z. Lu, Removal of phospho-head groups of membrane lipids immobilizes voltage sensors of K^+ channels, Nature 451 (2008) 826–829.
[26] S. Brauchi, G. Orta, C. Mascayano, M. Salazar, N. Raddatz, H. Urbina, et al., Dissection of the components for PIP2 activation and thermosensation in TRP channels, Proc. Natl. Acad. Sci. U. S. A. 104 (2007) 10246–10251.
[27] G.E. Flynn, W.N. Zagotta, Molecular mechanism underlying phosphatidylinositol 4,5-bisphosphate-induced inhibition of SpIH channels, J. Biol. Chem. 286 (2011) 15535–15542.
[28] S.B. Hansen, X. Tao, R. MacKinnon, Structural basis of PIP2 activation of the classical inward rectifier K^+ channel Kir2.2, Nature 477 (2011) 495–498.
[29] C.L. Huang, S. Feng, D.W. Hilgemann, Direct activation of inward rectifier potassium channels by PIP2 and its stabilization by Gbetagamma, Nature 391 (1998) 803–806.
[30] M. Kruse, G.R.V. Hammond, B. Hille, Regulation of voltage-gated potassium channels by PI(4,5)P2, J. Gen. Physiol. 140 (2012) 189–205.
[31] D.E. Logothetis, V.I. Petrou, S.K. Adney, R. Mahajan, Channelopathies linked to plasma membrane phosphoinositides, Pflügers Arch. Eur. J. Physiol. 460 (2010) 321–341.
[32] N. Rodriguez, M.Y. Amarouch, J. Montnach, J. Piron, A.J. Labro, F. Charpentier, et al., Phosphatidylinositol-4,5-bisphosphate (PIP(2)) stabilizes the open pore conformation of the Kv11.1 (hERG) channel, Biophys. J. 99 (2010) 1110–1118.
[33] B.-C. Suh, B. Hille, PIP2 is a necessary cofactor for ion channel function: how and why? Annu. Rev. Biophys. 37 (2008) 175–195.
[34] M.R. Whorton, R. MacKinnon, Crystal structure of the mammalian GIRK2 K^+ channel and gating regulation by G proteins, PIP2, and sodium, Cell 147 (2011) 199–208.
[35] H. Zhang, L.C. Craciun, T. Mirshahi, T. Rohacs, C.M.B. Lopes, T. Jin, et al., PIP(2) activates KCNQ channels, and its hydrolysis underlies receptor-mediated inhibition of M currents, Neuron 37 (2003) 963–975.
[36] M.A. Zaydman, J.R. Silva, K. Delaloye, Y. Li, H. Liang, H.P. Larsson, et al., Kv7.1 ion channels require a lipid to couple voltage sensing to pore opening, Proc. Natl. Acad. Sci. 110 (2013) 13180–13185.
[37] L. Stephens, A. McGregor, P. Hawkins, Phosphoinositide-3-kinases — regulation by cell surface receptors and function of 3-phosphorylated lipids, in: S. Cockcroft (Ed.), Biol. Phosphoinositides, Oxford University Press, Oxford, UK, 2000, pp. 32–107.
[38] F. Abderemane-Ali, Z. Es-Salah-Lamoureux, L. Delemotte, M.A. Kasimova, A.J. Labro, D.J. Snyders, et al., Dual effect of phosphatidyl (4,5)-bisphosphate PIP2 on Shaker K^+ channels, J. Biol. Chem. 287 (2012) 36158–36167.
[39] A.A. Rodriguez-Menchaca, S.K. Adney, Q.-Y. Tang, X.-Y. Meng, A. Rosenhouse-Dantsker, M. Cui, et al., PIP2 controls voltage-sensor movement and pore opening of Kv channels through the S4–S5 linker, Proc. Natl. Acad. Sci. U. S. A. 109 (2012) E2399–E2408.
[40] C.E. Morris, Voltage-gated channel mechanosensitivity: fact or friction? Front. Physiol. 2 (2011) 25.
[41] I.V. Tabarean, C.E. Morris, Membrane stretch accelerates activation and slow inactivation in Shaker channels with S3–S4 linker deletions, Biophys. J. 82 (2002) 2982–2994.
[42] U. Laitko, C.E. Morris, Membrane tension accelerates rate-limiting voltage-dependent activation and slow inactivation steps in a Shaker channel, J. Gen. Physiol. 123 (2004) 135–154.
[43] L. Martínez, R. Andrade, E.G. Birgin, J.M. Martínez, PACKMOL: a package for building initial configurations for molecular dynamics simulations, J. Comput. Chem. 30 (2009) 2157–2164.
[44] A.D. Mackerell Jr., M. Feig, C.L. Brooks III, Extending the treatment of backbone energetics in protein force fields: limitations of gas-phase quantum mechanics in reproducing protein conformational distributions in molecular dynamics simulations, J. Comput. Chem. 25 (2004) 1400–1415.
[45] W.L. Jorgensen, J. Chandrasekhar, J.D. Madura, R.W. Impey, M.L. Klein, Comparison of simple potential functions for simulating liquid water, J. Chem. Phys. 79 (1983) 926.
[46] M.T. Hyvönen, P.T. Kovanen, Molecular dynamics simulation of sphingomyelin bilayer, J. Phys. Chem. B 107 (2003) 9102–9108.
[47] J.B. Klauda, R.M. Venable, J.A. Freites, J.W. O'Connor, D.J. Tobias, C. Mondragon-Ramirez, et al., Update of the CHARMM all-atom additive force field for lipids: validation on six lipid types, J. Phys. Chem. B 114 (2010) 7830–7843.
[48] D. Lupyan, M. Mezei, D.E. Logothetis, R. Osman, A molecular dynamics investigation of lipid bilayer perturbation by PIP2, Biophys. J. 98 (2010) 240–247.
[49] J.C. Phillips, R. Braun, W. Wang, J. Gumbart, E. Tajkhorshid, E. Villa, et al., Scalable molecular dynamics with NAMD, J. Comput. Chem. 26 (2005) 1781–1802.

[50] L. Delemotte, F. Dehez, W. Treptow, M. Tarek, Modeling membranes under a transmembrane potential, J. Phys. Chem. B 112 (2008) 5547–5550.
[51] W. Treptow, M. Tarek, M.L. Klein, Initial response of the potassium channel voltage sensor to a transmembrane potential, J. Am. Chem. Soc. 131 (2009) 2107–2109.
[52] E. Stefani, L. Toro, E. Perozo, F. Bezanilla, Gating of Shaker K^+ channels: I. Ionic and gating currents, Biophys. J. 66 (1994) 996–1010.
[53] J.-X. Cheng, S. Pautot, D.A. Weitz, X.S. Xie, Ordering of water molecules between phospholipid bilayers visualized by coherent anti-Stokes Raman scattering microscopy, Proc. Natl. Acad. Sci. 100 (2003) 9826–9830.
[54] L. Delemotte, M. Tarek, Molecular dynamics simulations of lipid membrane electroporation, J. Membr. Biol. 245 (2012) 531–543.
[55] K. Gawrisch, D. Ruston, J. Zimmerberg, V.A. Parsegian, R.P. Rand, N. Fuller, Membrane dipole potentials, hydration forces, and the ordering of water at membrane surfaces, Biophys. J. 61 (1992) 1213–1223.
[56] W. Shinoda, M. Shimizu, S. Okazaki, Molecular dynamics study on electrostatic properties of a lipid bilayer: polarization, electrostatic potential, and the effects on structure and dynamics of water near the interface, J. Phys. Chem. B 102 (1998) 6647–6654.
[57] L. Delemotte, M. Tarek, Electroporation of lipid membranes, in: A. Pakhomov, D. Miklavcic, M. Markov (Eds.), Adv. Electroporation Tech. Biol. Med, Taylor and Francis/CRC Press, 2010, pp. 141–160.
[58] M.L. Berkowitz, D.L. Bostick, S. Pandit, Aqueous solutions next to phospholipid membrane surfaces: insights from simulations, Chem. Rev. 106 (2006) 1527–1539.
[59] R.J. Mashl, H.L. Scott, S. Subramaniam, E. Jakobsson, Molecular simulation of dioleoylphosphatidylcholine lipid bilayers at differing levels of hydration, Biophys. J. 81 (2001) 3005–3015.
[60] J.N. Sachs, P.S. Crozier, T.B. Woolf, Atomistic simulations of biologically realistic transmembrane potential gradients, J. Chem. Phys. 121 (2004) 10847–10851.
[61] A.M. Smondyrev, M.L. Berkowitz, Structure of dipalmitoylphosphatidylcholine/cholesterol bilayer at low and high cholesterol concentrations: molecular dynamics simulation, Biophys. J. 77 (1999) 2075–2089.
[62] A.M. Thomas, S.C. Harmer, T. Khambra, A. Tinker, Characterization of a binding site for anionic phospholipids on KCNQ1, J. Biol. Chem. 286 (2011) 2088–2100.
[63] M.R. Schmidt, P.J. Stansfeld, S.J. Tucker, M.S.P. Sansom, Simulation-based prediction of phosphatidylinositol 4,5-bisphosphate binding to an ion channel, Biochemistry (Mosc) 52 (2013) 279–281.
[64] M.A. Zaydman, J.R. Silva, K. Delaloye, H.P. Larsson, J. Cui, The role of PIP2 in the voltage-dependent activation of Kv7.1, Biophys. J. 102 (2012) 331a–332a.